
Article:
Berry, T. A., Podolyák, Zs, Carroll, R. J. et al. (2020) Octupole states in Tl 207 studied through β decay. Physical Review C. 054311. ISSN: 2469-9993

https://doi.org/10.1103/PhysRevC.101.054311

Octupole states in ^{207}Tl studied through β decay

T. A. Berry,[1] Zs. Podolyák,[1,*] R. J. Carroll,[1] R. Lică,[2,3] B. A. Brown,[4] H. Grawe,[5] Ch. Sotty,[3,6] N. K. Timofeyuk,[1] T. Alexander,[1] A. N. Andreyev,[7] S. Ansari,[8] M. J. G. Borge,[2] M. Brunet,[1] J. R. Cresswell,[9] C. Fahlander,[10] L. M. Fraile,[11] H. O. U. Fynbo,[12] E. Gamba,[13] W. Gelletly,[1] R.-B. Gerst,[8] M. Górska,[5] A. Gredley,[9] P. Greenlees,[14,15] L. J. Harkness-Brennan,[9] M. Huyse,[6] S. M. Judge,[16] D. S. Judson,[9] J. Konki,[14,15,†] M. Kowalska,[2] J. Kurcewicz,[2] I. Kuti,[17] S. Lalkovski,[1] I. Lazarus,[18] M. Lund,[12] M. Madurga,[2] N. Mărginean,[3] R. Mărginean,[3] I. Marroquin,[19] C. Mihai,[3] R. E. Mihai,[3] E. Nácher,[19] A. Negret,[3] S. Nae,[3] C. Niţă,[3,13] S. Pascu,[3] R. D. Page,[9] Z. Patel,[1] A. Perea,[19] J. Phrompao,[20] M. Piersa,[21] V. Pucknell,[18] P. Rahkila,[14,15] E. Rapisarda,[2] P. H. Regan,[1,16] F. Rotaru,[3] M. Rudigier,[1] C. M. Shand,[1] R. Shearman,[1,16] E. C. Simpson,[22] S. Stegemann,[8] T. Stora,[2] O. Tengblad,[19] A. Turturica,[3] P. Van Duppen,[6] V. Vedia,[11] P. M. Walker,[1] N. Warr,[8] F. P. Wearing,[9] and H. De Witte[6]

[1]*Department of Physics, University of Surrey, Guildford, GU2 7XH, United Kingdom*
[2]*CERN, Physics Department, 1211 Geneva 23, Switzerland*
[3]*H. Hulubei National Institute for Physics and Nuclear Engineering, RO-077125 Bucharest, Romania*
[4]*Department of Physics and Astronomy and National Superconducting Cyclotron Laboratory, Michigan State University, East Lansing, Michigan 48824-1321, USA*
[5]*GSI Helmholtzzentrum für Schwerionenforschung GmbH, Planckstraße 1, 64291 Darmstadt, Germany*
[6]*KU Leuven, Instituut voor Kern- en Stralingsfysica, Celestijnenlaan 200D, 3001 Leuven, Belgium*
[7]*Department of Physics, University of York, York YO10 5DD, N Yorkshire, United Kingdom*
[8]*Institut für Kernphysik der Universität zu Köln, Zülpicher Straße 77, 50937 Köln, Germany*
[9]*Department of Physics, Oliver Lodge Laboratory, University of Liverpool, L69 7ZE Liverpool, United Kingdom*
[10]*Department of Physics, Lund University, S-22100 Lund, Sweden*
[11]*Grupo de Física Nuclear, FAMN, Universidad Complutense, CEI Moncloa, 28040 Madrid, Spain*
[12]*Department of Physics and Astronomy, Aarhus University, DK-8000 Aarhus, Denmark*
[13]*University of Brighton, Brighton BN2 4GJ, United Kingdom*
[14]*University of Jyvaskyla, Department of Physics, P.O. Box 35, FI-40014 University of Jyvaskyla, Finland*
[15]*Helsinki Institute of Physics, University of Helsinki, P.O. Box 64, FI-00014 Helsinki, Finland*
[16]*National Physical Laboratory, Teddington, Middlesex TW11 0LW, United Kingdom*
[17]*Institute of Nuclear Research of the Hungarian Academy of Sciences, 4026 Debrecen, Hungary*
[18]*STFC, Daresbury Laboratory, Warrington WA4 4AD, United Kingdom*
[19]*Instituto de Estructura de la Materia, CSIC, Serrano 113 bis, E-28006 Madrid, Spain*
[20]*Department of Physics and Materials Science, Chiang Mai University, 50200 Chiang Mai, Thailand*
[21]*Faculty of Physics, University of Warsaw, PL 02-093 Warsaw, Poland*
[22]*Department of Nuclear Physics, Research School of Physics, The Australian National University, Canberra ACT 2600, Australia*

(Received 5 December 2019; revised manuscript received 16 March 2020; accepted 28 April 2020; published 18 May 2020)

The β decay of ^{207}Hg into the single-proton-hole nucleus ^{207}Tl has been studied through γ-ray spectroscopy at the ISOLDE Decay Station (IDS) with the aim of identifying states resulting from coupling of the $\pi s_{1/2}^{-1}$, $\pi d_{3/2}^{-1}$, and $\pi h_{11/2}^{-1}$ shell model orbitals to the collective octupole vibration. Twenty-two states were observed lying between 2.6 and 4.0 MeV, eleven of which were observed for the first time, and 78 new transitions were placed. Two octupole states ($s_{1/2}$-coupled) are identified and three more states ($d_{3/2}$-coupled) are tentatively assigned using spin-parity inferences, while further $h_{11/2}$-coupled states may also have been observed for the first time. Comparisons are made with state-of-the-art large-scale shell model calculations and previous observations made in this region, and systematic underestimation of the energy of the octupole vibrational states is noted. We suggest that in order to resolve the difference in predicted energies for collective and noncollective $t = 1$

*Corresponding author: z.podolyak@surrey.ac.uk
†Present address: CERN, CH-1211 Geneva 23, Switzerland.

states (t is the number of nucleons breaking the ^{208}Pb core), the effect of $t = 2$ mixing may be reduced for octupole-coupled states. The inclusion of mixing with $t = 0, 2, 3$ excitations is necessary to replicate all $t = 1$ state energies accurately.

DOI: 10.1103/PhysRevC.101.054311

I. INTRODUCTION

One of the most prominent features of the well-studied stable doubly-magic ^{208}Pb nucleus is its octupole vibrational first excited state at an energy of 2614.5 keV with a reduced transition strength $B(E3; 3^- \rightarrow 0^+) = 33.8(6)$ W.u. [1]. The excitation arises as a result of the collective behavior of a number of $\Delta l = \Delta j = 3$ particle-hole excitations across the proton and neutron closed shells. Such collective octupole excitations are observed in a number of neighboring nuclei [2,3], including the single-proton-hole nucleus ^{207}Tl [4].

It is expected that the composition of the collective octupole excitation in terms of shell model wave functions is reflected in its behavior when coupling to those orbitals. Knowledge of the composition of this phonon is of interest. While large-scale shell model calculations are able to describe the collective octupole and double-octupole states around ^{208}Pb [4,5], the energies of the octupole states are not reproduced accurately, indicating a possible gap in our knowledge. Experimental data on coupled states are therefore needed. The single-proton-hole nucleus ^{207}Tl is expected to feature a number of states resulting from coupling between the octupole phonon and the $\pi s_{1/2}^{-1}$, $\pi d_{3/2}^{-1}$, and $\pi h_{11/2}^{-1}$ states in the 2–4 MeV energy region. The capability of β decay to populate a number of excited states in the 2.5–4.0 MeV energy region [6] means that β^- decay from the parent nucleus ^{207}Hg ($J^\pi_{\text{g.s.}} = (9/2^+)$, $Q_\beta = 4550(30)$ keV [7,8]) should populate a number of these coupled states in allowed and first-forbidden decays.

The β decay of ^{207}Hg has been studied once before [6] and a level scheme was produced. The scheme includes the four states lowest in energy corresponding to the single-proton-hole states (lowest to highest in energy) $\pi 3s_{1/2}^{-1}$, $\pi 2d_{3/2}^{-1}$, $\pi 1h_{11/2}^{-1}$, and $\pi 2d_{5/2}^{-1}$. Above these states lie a number of uncharacterized states expected to result from coupling between those low-lying single-particle states and the 3^-, 4^-, and 5^- excitations observed in ^{208}Pb. Fifteen states, up to an energy of 3592 keV, and 32 transitions were observed [6]. In addition, a state containing significant $\pi 1g_{7/2}^{-1}$ strength has been placed at 3474(6) keV in a number of particle transfer experiments [9–15]. Also, a deep-inelastic reaction experiment [4] observed a number of high-spin yrast and near-yrast states with excitation energies between 3.8 and 7.0 MeV, including the 3813 keV $17/2^+$ $\pi h_{11/2}^{-1} \times 3^-$ octupole-coupled state.

II. EXPERIMENTAL DETAILS

Two experiments took place at the CERN-ISOLDE facility. In both experiments, a molten lead target coupled to a VD5 FEBIAD [16] ion source was bombarded by a 1.4 GeV beam of protons and singly-charged ^{207}Hg was extracted. The reaction mechanism of ^{207}Hg production is not clear. A secondary $(n, 2p)$ reaction was assumed previously [6]. However, more recent population of $N > 126$ nuclei using a thin target [17] suggests an alternative production mechanism, where the role of the Δ resonance [18] should be considered. While the reaction mechanism leading to the population of ^{207}Hg does not affect the results presented here, its understanding is important for planning future experiments.

In the first experiment the beam was extracted down the ISOLDE beam line with a potential of 30 kV. Ions with mass $A = 207$ were selected by the General Purpose Separator (GPS) and deposited upon the tape at the ISOLDE Decay Station (IDS), at a rate of up to 5×10^4 pps. The four resident four-crystal high-purity germanium (HPGe) clover detectors were combined with a single Miniball cluster detector [19] along the beam axis for improved total γ efficiency (22% at 100 keV, 8% at 1 MeV). Three plastic scintillator detectors were used for β gating (total β efficiency $\approx$ 30%). In the second experiment, aimed at $\gamma\gamma$ angular correlation measurements, the beam was extracted at 50 kV, separated with GPS and deposited at IDS at a higher rate of up to 2×10^5 pps. The four IDS clovers were combined with a fifth (TIGRESS [20]) clover positioned of axis (total γ efficiency 11% at 100 keV, 4% at 1 MeV). β gating using a plastic scintillating block and photomultiplier tube surrounding the tape was switched off during the experiment as high count rates led to significant dead time. The triggerless total data readout (TDR) system [21] at IDS was used for data acquisition.

Efficiency calibration of the array of germanium detectors was performed using ^{152}Eu and ^{60}Co sources. Extension of this calibration up to an energy of 2614 keV utilized the known ratio [1] between the intensities of the 583 and 2614 keV transitions in ^{208}Pb following β^- decay of ^{208}Tl on the tape, measured during a separate run on the $A = 208$ separator setting. For angular correlations the relative efficiencies of individual detectors must be known to a high precision. Individual detectors were efficiency calibrated as above, and were further calibrated by adjusting for relative peak intensities of ungated single transitions in ^{207}Tl measured during the run.

Matrices of $\beta\gamma$ and $\beta\gamma\gamma$ coincidences were obtained using data from the first experiment. These were used to establish transition energies and intensities. The effect of the condition of β detection on the determined γ-ray intensities was investigated, and no systematics bias was found. Intensity balances could also be used to determine log ft values for each state.

In order to characterize observed states, spin-parity assignments must be made. Angular correlation measurements are one method and have not previously been performed at the IDS. The probability distribution for emission of a γ ray at an angle θ relative to a coincident γ ray directly preceding or

TABLE I. Number of crystal-crystal pairs per 5° angular bin for the asymmetric five-clover detector configuration at IDS, used here for angular correlation measurements. Angles are symmetric around 90°, so, e.g., 0°–5° also includes 175°–180°.

Angle	0°–5°	5°–10°	10°–15°	15°–20°	20°–25°	25°–30°
Pairs	0	1	2	1	1	3
	30°–35°	35°–40°	40°–45°	45°–50°	50°–55°	55°–60°
	3	7	10	2	14	12
	60°–65°	65°–70°	70°–75°	75°–80°	80°–85°	85°–90°
	15	8	19	24	18	20

following it is given by the equation

$$W(\theta) = \sum_{\text{even } k}^{k_{\max}} A_k Q_k P_k(\cos\theta), \tag{1}$$

where, for $I_1 \xrightarrow{L_1+L_1'} I_2 \xrightarrow{L_2+L_2'} I_3$ (L is the angular momentum of the photon) k is an even integer for which $k_{\max} = \min(2I_2, 2L_1', 2L_2')$, $P_k(\cos\theta)$ are Legendre polynomials, Q_k are solid angle correction coefficients, and A_k are the angular correlation coefficients which can be related to the spins, multipolarities, and mixing ratios through angular momentum considerations (see Ref. [22]). Here $k > 4$ is safely ignored. Fits of $W(\theta)$ normalised to A_0 may be compared with theoretical A_2, A_4 values to support or rule out certain combinations of level spins. The added degrees of freedom caused by mixing mean that the method is most effective when applied to stretched electric transitions, which can generally be assumed to be unmixed.

Angular correlation measurements were performed using data from the second experiment (five clover detectors) in order to support spin-parity assignments. Correlations were calculated between individual HPGe crystals in order to reduce solid angle spreading and increase the number of detector-detector angles. Placing the fifth detector off axis reduced the symmetry of the system and as a result gave an increase in the number of angles. The angles available in the data set of 320 crystal-crystal pairs are summarized in Table I. Add-back was performed by assuming the crystal of greatest energy deposition to be the initial point of interaction of the γ ray. The solid angle correction coefficients Q_k were calculated using the integration method [23], and the approach was verified using coincidences in the decay of ^{152}Eu. More details are given in Ref. [24].

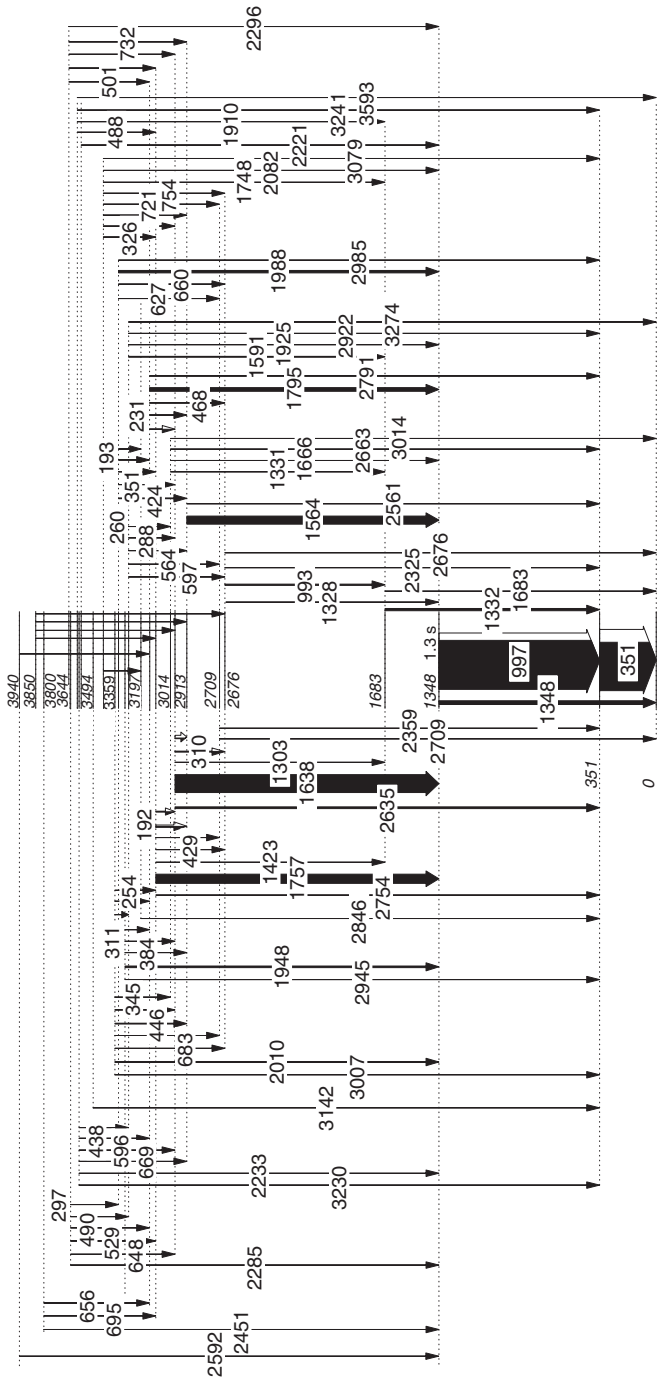

FIG. 1. Level scheme for ^{207}Tl observed in this work.

III. RESULTS

A level scheme for ^{207}Tl below $Q_\beta = 4550(30)$ keV has been built using β-gated γ and $\gamma\gamma$ coincidence spectra. The full level scheme is shown in Fig. 1, and the full list of observed transitions and intensities is recorded in Table II. Data from the 2014 experiment were used due to the comparatively lower level of background in the spectra and the ability to gate on β signals, further improving the quality of the spectra. Examples of γ-ray spectra in coincidences with the 351 and 1683 keV transitions are shown in Fig. 2. Transitions were verified by cross-comparison with the 2016 data. All possible transitions between states were analyzed in coincidence spectra. As well as observing fifteen previously known states [7], eleven new states and 78 new transitions have been placed in this analysis. These states lie at energies of 3013.8, 3197.3, 3430.5, 3493.6, 3569.7, 3581.3, 3633.6, 3644.2, 3800.0, 3850.0, and 3940.3 keV. The states at 3634 and 3644 keV were tentatively suggested in the previous β-decay work [6].

Electron conversion coefficients are dependent on transition multipolarities and multipolarity mixing ratios. It is

TABLE II. Full list of transitions observed in ^{207}Tl in this analysis. $I_{\gamma,\text{rel.}}$ is the relative intensity of the γ-ray emission (without electron conversion correction) with respect to intensity 100 for the 351 keV transition populating the ground state. $B_{\text{est.}}(\sigma L)$ is the calculated Weisskopf strength of a given transition assuming a certain "typical" strength (written in bold) for a different transition depopulating the same state. For details see text.

E_i (keV)	J_i^π	E_f (keV)	J_f^π	E_γ (keV)	σL	$I_{\gamma,\text{rel.}}$	$B_{\text{est.}}(\sigma L)$ (W.u.)
351.2	$3/2^+$	0.0	$1/2^+$	351.2(2)	$M1$	100(5)	
1348.3	$11/2^-$	351.2	$3/2^+$	997.2(2)	$M4$	103(7)	
		0.0	$1/2^+$	1348.2(2)	$E5$	8.4(6)	
1682.8	$5/2^+$	351.2	$3/2^+$	1331.8(2)	$M1$	4.8(4)	0.08
		0.0	$1/2^+$	1682.8(3)	$E2$	0.93(8)	**1.0**
2676.0	$7/2^-$	1682.8	$5/2^+$	993.4(2)	$E1$	2.9(2)	3×10^{-4}
		1348.3	$11/2^-$	1328.1(3)	$E2$	0.37(4)	0.3
		351.2	$3/2^+$	2324.9(3)	$M2$	0.079(8)	0.5
		0.0	$1/2^+$	2676.1(4)	$E3$	0.14(1)	**30**
2709.3	$5/2^-$	351.2	$3/2^+$	2358.6(3)	$E1$	0.28(3)	$\mathbf{1 \times 10^{-4}}$
		0.0	$1/2^+$	2708.5(5)	$M2$	0.012(3)	2.0
2912.6	$(9/2^-)$	1348.3	$11/2^-$	1564.2(3)	$(M1)$	20(2)	2×10^{-4}
		351.2	$3/2^+$	2561.4(3)	$(E3)$	0.70(7)	**1**
2985.8	$(9/2^-)$	2912.6	$(9/2^-)$	73(1)	$(M1)$	1.2(3)	0.9
		2676.0	$7/2^-$	309.7(2)	$(M1)$	1.6(1)	0.02
		1682.8	$5/2^+$	1302.8(2)	$(M2)$	0.064(8)	0.2
		1348.3	$11/2^-$	1637.5(3)	$(M1)$	44(4)	3×10^{-3}
		351.2	$3/2^+$	2634.6(4)	$(E3)$	4.6(5)	**30**
3013.8	$(7/2^-)$	1682.8	$5/2^+$	1331.2(2)	$(E1)$	0.60(5)	$\mathbf{1 \times 10^{-4}}$
		1348.3	$11/2^-$	1665.6(3)	$(E2)$	0.11(1)	0.1
		351.2	$3/2^+$	2662.6(4)	$(M2)$	0.037(4)	0.5
		0.0	$1/2^+$	3013.6(5)	$(E3)$	0.0024(6)	1
3104.9	$(9/2^-)$	2985.8	$(9/2^-)$	119.1(2)	$(M1)$	0.22(5)	7×10^{-3}
		2912.6	$(9/2^-)$	192.4(2)	$(M1)$	1.17(6)	9×10^{-3}
		2709.3	$5/2^-$	395.9(3)	$(E2)$	0.006(2)	0.01
		2676.0	$7/2^-$	428.7(2)	$(M1)$	0.33(2)	2×10^{-4}
		1682.8	$5/2^+$	1423.2(4)	$(M2)$	0.014(7)	5×10^{-3}
		1348.3	$11/2^-$	1756.6(3)	$(M1)$	23(2)	2×10^{-4}
		351.2	$3/2^+$	2753.6(4)	$(E3)$	1.0(1)	**1**
3143.2	$(9/2^-)$	2985.8	$(9/2^-)$	157.7(2)	$(M1)$	0.45(3)	0.7
		2912.6	$(9/2^-)$	231.1(2)	$(M1)$	0.69(4)	0.3
		2676.0	$7/2^-$	467.5(3)	$(M1)$	0.019(3)	1×10^{-3}
		1348.3	$11/2^-$	1795.2(3)	$(M1)$	9.1(8)	0.01
		351.2	$3/2^+$	2791.4(5)	$(E3)$	0.010(2)	**1**
3197.3	$(5/2^-)$	351.2	$3/2^+$	2846.1(4)	$(E1)$	0.006(1)	$--$
3273.5	$(7/2^-)$	3013.8	$(7/2^-)$	259.6(2)	$(M1)$	0.24(1)	0.3
		2985.8	$(9/2^-)$	287.7(2)	$(M1)$	0.101(6)	0.09
		2912.6	$(9/2^-)$	361.0(2)	$(M1)$	0.015(2)	7×10^{-3}
		2709.3	$5/2^-$	563.7(2)	$(M1)$	0.18(2)	0.02
		2676.0	$7/2^-$	597.3(2)	$(M1)$	0.098(8)	0.01
		1682.8	$5/2^+$	1590.6(3)	$(E1)$	2.2(2)	$\mathbf{1 \times 10^{-4}}$
		1348.3	$11/2^-$	1925.4(3)	$(E2)$	0.010(2)	3×10^{-3}
		351.2	$3/2^+$	2922.0(4)	$(M2)$	0.081(9)	0.3
		0.0	$1/2^+$	3273.8(4)	$(E3)$	0.018(3)	2
3296.2	$(9/2^-)$	3143.2	$(9/2^-)$	152.7(2)	$(M1)$	0.024(2)	0.1
		2985.8	$(9/2^-)$	310.5(2)	$(M1)$	0.12(1)	0.07
		2912.6	$(9/2^-)$	383.6(2)	$(M1)$	0.035(3)	0.01
		1348.3	$11/2^-$	1947.9(3)	$(M1)$	3.9(3)	9×10^{-3}
		351.2	$3/2^+$	2944.5(6)	$(E3)$	0.005(1)	**1**

TABLE II. (*Continued.*)

E_i (keV)	J_i^π	E_f (keV)	J_f^π	E_γ (keV)	σL	$I_{\gamma,\mathrm{rel.}}$	$B_{\mathrm{est.}}(\sigma L)$ (W.u.)
3336.5	$(9/2^-)$	3197.3	$(5/2^-)$	139.8(4)	$(E2)$	0.0018(5)	5
		3143.2	$(9/2^-)$	192.8(2)	$(M1)$	0.17(1)	0.01
		3104.9	$(9/2^-)$	231.6(2)	$(M1)$	0.17(1)	7×10^{-3}
		2985.8	$(9/2^-)$	350.8(2)	$(M1)$	0.51(3)	6×10^{-3}
		2912.6	$(9/2^-)$	423.9(2)	$(M1)$	0.84(5)	5×10^{-3}
		2709.3	$5/2^-$	626.8(3)	$(E2)$	0.017(2)	0.03
		2676.0	$7/2^-$	660.4(2)	$(M1)$	0.17(1)	3×10^{-4}
		1348.3	$11/2^-$	1988.0(3)	$(M1)$	6.1(5)	4×10^{-4}
		351.2	$3/2^+$	2985.3(4)	$(E3)$	0.20(2)	**1**
3358.7	$(9/2^-)$	3273.5	$(7/2^-)$	85.3(5)	$(M1)$	0.008(2)	0.2
		3143.2	$(9/2^-)$	215.3(2)	$(M1)$	0.047(3)	0.07
		3104.9	$(9/2^-)$	254.1(2)	$(M1)$	0.24(2)	0.2
		3013.8	$(7/2^-)$	345.2(3)	$(M1)$	0.08(2)	0.03
		2985.8	$(9/2^-)$	373.0(2)	$(M1)$	0.063(5)	0.02
		2912.6	$(9/2^-)$	446.3(2)	$(M1)$	1.5(1)	0.3
		2709.3	$5/2^-$	649.5(5)	$(E2)$	0.003(1)	0.1
		2676.0	$7/2^-$	682.6(2)	$(M1)$	0.16(1)	8×10^{-3}
		1348.3	$11/2^-$	2010.5(3)	$(M1)$	2.5(2)	5×10^{-3}
		351.2	$3/2^+$	3007.3(4)	$(E3)$	0.0066(9)	**1**
3430.5	$(7/2^-)$	3197.3	$(5/2^-)$	234.0(4)	$(M1)$	0.0011(4)	0.1
		3104.9	$(9/2^-)$	325.8(2)	$(M1)$	0.038(3)	1
		2985.8	$(9/2^-)$	444.7(2)	$(M1)$	0.034(4)	0.5
		2912.6	$(9/2^-)$	518.1(2)	$(M1)$	0.039(4)	0.3
		2709.3	$5/2^-$	720.7(2)	$(M1)$	0.052(4)	0.2
		2676.0	$7/2^-$	754.1(2)	$(M1)$	0.058(5)	0.2
		1682.8	$5/2^+$	1747.8(4)	$(E1)$	0.05(1)	$\mathbf{1 \times 10^{-4}}$
		1348.3	$11/2^-$	2082.2(3)	$(E2)$	0.63(6)	7
		351.2	$3/2^+$	3079.2(4)	$(M2)$	0.0052(9)	0.9
3493.6	$(5/2^-,7/2)$	351.2	$3/2^+$	3142.4(4)		0.008(1)	
3569.7	$(11/2^-)$	1348.3	$11/2^-$	2221.4(3)	$(M1)$	0.17(2)	
3581.3	$(9/2^-)$	3273.5	$(7/2^-)$	307.8(2)	$(M1)$	0.0069(6)	0.02
		3143.2	$(9/2^-)$	437.7(2)	$(M1)$	0.046(3)	0.04
		2985.8	$(9/2^-)$	595.6(2)	$(M1)$	0.061(5)	0.02
		2912.6	$(9/2^-)$	669.0(2)	$(M1)$	0.037(4)	8×10^{-3}
		1348.3	$11/2^-$	2232.9(3)	$(M1)$	0.10(1)	6×10^{-4}
		351.2	$3/2^+$	3230.2(5)	$(E3)$	0.0025(6)	**1**
3592.4	$(7/2^-)$	3104.9	$(9/2^-)$	488.3(3)	$(M1)$	0.006(1)	0.02
		1682.8	$5/2^+$	1909.7(3)	$(E1)$	0.17(1)	$\mathbf{1 \times 10^{-4}}$
		351.2	$3/2^+$	3241.0(4)	$(M2)$	0.0030(5)	0.2
		0.0	$1/2^+$	3593(1)	$(E3)$	0.0015(8)	2
3633.6	$(11/2^-)$	3336.5	$(9/2^-)$	296.6(3)	$(M1)$	0.038(8)	0.03
		3273.5	$(7/2^-)$	360.0(2)	$(E2)$	0.005(4)	7
		3143.2	$(9/2^-)$	490.0(2)	$(M1)$	0.059(4)	0.01
		3104.9	$(9/2^-)$	528.7(2)	$(M1)$	0.048(4)	8×10^{-3}
		2985.8	$(9/2^-)$	647.8(2)	$(M1)$	0.25(2)	0.02
		1348.3	$11/2^-$	2285.2(3)	$(M1)$	0.50(5)	$\mathbf{1 \times 10^{-3}}$
3644.2	$(11/2^-)$	3143.2	$(9/2^-)$	500.9(2)	$(M1)$	0.023(1)	7×10^{-3}
		3104.9	$(9/2^-)$	539.6(3)	$(M1)$	0.005(1)	1×10^{-3}
		2985.8	$(9/2^-)$	658.0(4)	$(M1)$	0.005(2)	6×10^{-4}
		2912.6	$(9/2^-)$	731.9(3)	$(M1)$	0.012(2)	1×10^{-3}
		1348.3	$11/2^-$	2296.1(3)	$(M1)$	0.33(3)	$\mathbf{1 \times 10^{-3}}$
3800.0[a]	(9/2, 11/2)	3143.2	$(9/2^-)$	656.2(2)	$(E1)$	0.025(2)	5×10^{-3}
		3104.9	$(9/2^-)$	695.8(4)	$(E1)$	0.0014(6)	2×10^{-4}
		1348.3	$11/2^-$	2451.3(3)	$(E1)$	0.027(3)	$\mathbf{1 \times 10^{-4}}$

TABLE II. (*Continued*.)

E_i (keV)	J_i^π	E_f (keV)	J_f^π	E_γ (keV)	σL	$I_{\gamma,\mathrm{rel.}}$	$B_{\mathrm{est.}}(\sigma L)$ (W.u.)
3850.0[a]	(7/2, 9/2)	3104.9	$(9/2^-)$	745.1(4)	$(E1)$	0.003(1)	8×10^{-5}
		2985.8	$(9/2^-)$	864.4(5)	$(E1)$	0.008(2)	1×10^{-4}
		2912.6	$(9/2^-)$	937.9(3)	$(E1)$	0.0022(7)	3×10^{-5}
		2676.0	$7/2^-$	1173.8(6)	$(E1)$	0.015(6)	$\mathbf{1 \times 10^{-4}}$
3940.3[a]	(9/2, 11/2)	3143.2	$(9/2^-)$	796.9(2)	$(E1)$	0.017(1)	2×10^{-3}
		1348.3	$11/2^-$	2592.2(3)	$(E1)$	0.024(3)	$\mathbf{1 \times 10^{-4}}$

[a]Positive parity is assumed for branching ratio calculations.

possible to infer conversion ratios indirectly by gating on the initial gamma ray in a γ–γ–γ cascade and attributing any intensity imbalance after correcting for efficiency between the second and third transitions to electron conversion. From the 1591–1332–351 keV and 1910–1332–351 keV coincidences we obtain the total internal conversion coefficient $\alpha(351.2\ \mathrm{keV}) = 0.23(5)$. The result is in agreement with a previous result $\alpha_K(351.2\ \mathrm{keV}) = 0.2041(37)$ measured by Gorodetzky *et al.* [25], and corresponds to the mixing ratiob $|\delta_{M1+E2}(351.2\ \mathrm{keV})| \leqslant 0.8$.

Values of $\log ft$ have been calculated for each observed state, taking into account ingoing and outgoing internal transition intensies (conversion-corrected [26] assuming zero mixing, except in the case of the 351.2 keV transition where the measured value is used) and assuming that the remainder populating intensity comes from direct β-decay population. A spin and parity of $J^\pi = (9/2^+)$ is assumed for the decaying ground state of ^{207}Hg [7]. The results are shown in Table III. These are used to support spin-parity assignments given their close empirical relation to the degree of forbiddenness of a decay [27].

Transition strengths in terms of the single-particle Weisskopf estimates may be calculated exactly but this requires a knowledge of level lifetimes. However, if the single-particle strength of one transition depopulating a state can be assumed, the relative strengths of other transitions depopulating the same state may be deduced using the relative intensities. These assumed strengths take into account the systematics of this region in the nuclear chart. The magnetic transitions do not exhibit any useful trends, but the electric transitions do, as described in the following paragraph.

Several $E1$ transitions connecting single-particle and octupole states have been observed in the neighboring ^{207}Pb [28] and ^{209}Bi [29] nuclei. All measured $B(E1)$ transition strengths are in the range of 10^{-3}–10^{-5} W.u., and so $B(E1) = 10^{-4}$ W.u. is used as an approximation. $E2$ transitions have strengths of roughly 0.1–3 W.u. [7,29,30] and so $B(E2) = 1.0$ W.u. is used. The 2614.5 keV octupole transition in ^{208}Pb has an established strength $B(E3) = 33.8(6)$ W.u. [1] and is observed with similar strength in nearby one- and two-particle nuclei, while noncollective $E3$ transitions have strengths within an order of magnitude of 1 W.u. [7,29,30]. Therefore in this work $B(E3) = 30$ W.u. is used for assigned collective octupole transitions, and $B(E3) = 1$ W.u. is used for noncollective octupole transitions.

The relative transition strength estimates are shown in Table II, with bold values indicating the assumed strength. Spin-parity assignments which give unphysically large transition strengths using this method have been ruled out.

IV. EXPERIMENTAL SPIN-PARITY ASSIGNMENTS

We discuss the spin-parity assignment for each state individually. These are largely based on experimental considerations. The branching ratios (and consequently the relative transition strengths) are considered. Realistically, in the absence of isomers, only $E1$, $M1$, $E2$, $M2$, and $E3$ transitions can occur, with $M2$ and $E3$ transitions only at high energies ($\gtrsim$1 MeV). We note that the $E3$ transition strength can be

TABLE III. Tabulation of calculated $\log ft$ results for all levels of ^{207}Tl observed in this work. For states which allow zero population within uncertainties, a lower $\log ft$ limit is used. The spin-parity of the parent ^{207}Hg nucleus is $(9/2^+)$ [7].

Level energy (keV)	J^π	I_β (%)	$\log ft$
0.0	$1/2^+$	0	
351.2(2)	$3/2^+$	−5(9)	
1348.3(2)	$11/2^-$	11(7)	7.2(4)
1682.8(2)	$5/2^+$	−0.1(3)	
2676.0(2)	$7/2^-$	0.3(2)	7.8(3)
2709.3(6)	$5/2^-$	0.02(2)	>8.7
2912.6(3)	$(9/2^-)$	6(2)	6.3(2)
2985.8(3)	$(9/2^-)$	40(5)	5.42(7)
3013.8(3)	$(7/2^-)$	0.21(5)	7.7(2)
3104.9(3)	$(9/2^-)$	21(3)	5.58(8)
3143.2(3)	$(9/2^-)$	8(1)	5.95(7)
3197.3(5)	$(5/2^-)$	0.001(1)	>9.5
3273.5(2)	$(7/2^-)$	2.3(3)	6.34(8)
3296.2(3)	$(9/2^-)$	3.2(4)	6.17(8)
3336.5(2)	$(9/2^-)$	6.5(6)	5.81(7)
3358.7(2)	$(9/2^-)$	3.8(4)	6.01(7)
3430.5(2)	$(7/2^-)$	0.70(8)	6.65(8)
3493.6(5)	$(5/2^-, 7/2)$	0.0060(9)	8.63(9)
3569.7(4)	(11/2)	0.12(2)	7.21(10)
3581.3(2)	$(9/2^-)$	0.20(2)	6.97(8)
3592.4(4)	$(7/2^-)$	0.14(2)	7.11(9)
3633.6(3)	$(11/2^-)$	0.70(8)	6.34(8)
3644.2(3)	$(11/2^-)$	0.28(4)	6.72(9)
3800.0(3)	(9/2, 11/2)	0.041(5)	7.27(9)
3850.0(4)	(7/2, 9/2)	0.022(6)	7.4(2)
3940.3(3)	(9/2, 11/2)	0.031(4)	7.08(10)

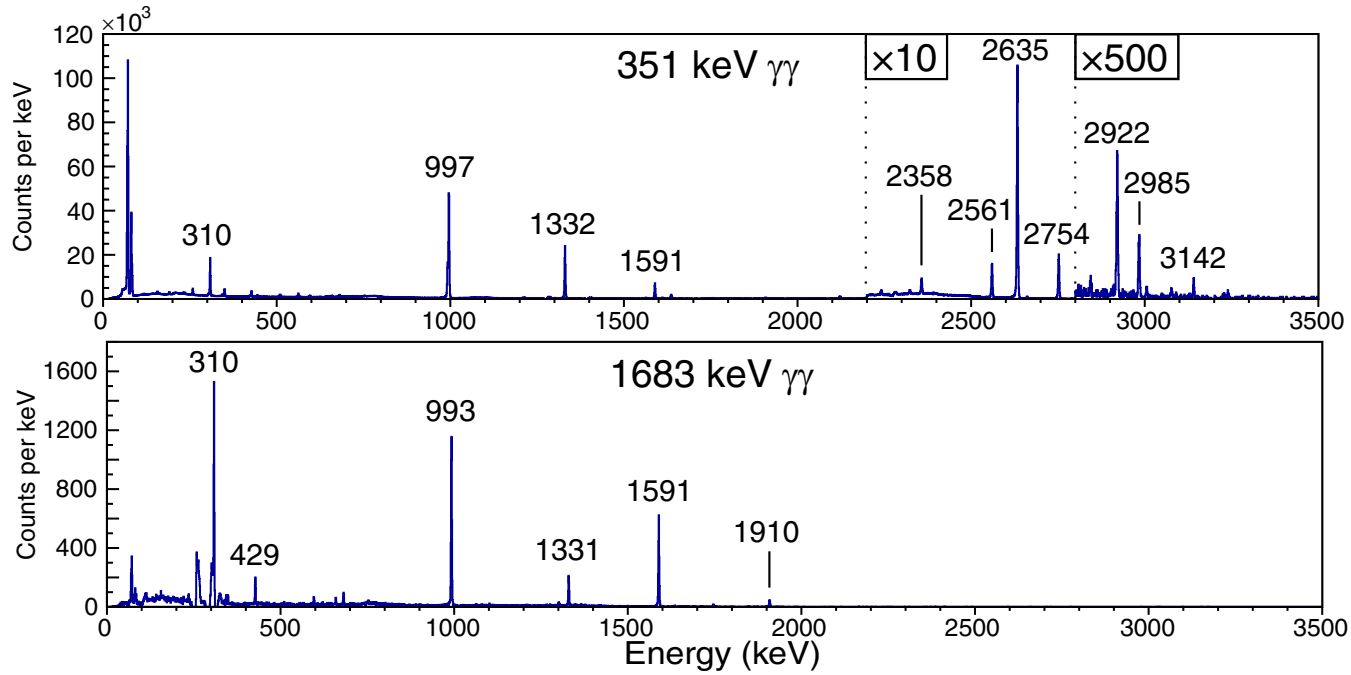

FIG. 2. β-gated γ-ray spectra, in coincidence with (top) the 351 keV $3/2^+ \rightarrow 1/2^+$ transition and (bottom) the 1683 keV $5/2^+ \rightarrow 1/2^+$ transition. Peak energies (keV) are labeled.

quite high: $B(E3) \approx 30$ W.u. [1] in this mass region due to the presence of the collective octupole phonon. The $\log ft$ results are also used, and are summarized in Table III. Often, theoretical considerations must be applied in spin-parity determination. Naïvely, the lowest-energy positive-parity states, other than the well-known single particle states, are expected at around 4 MeV arising from the coupling of the $h_{11/2}$ proton hole (1.348 MeV in ^{207}Tl) to the 3^- octupole phonon (2.614 MeV in ^{208}Pb). This is supported by the results of shell model calculations. As a result all states below 3.4 MeV are considered to have negative parity.

The 0, keV, keV, and 1683 keV states are single-particle states with well-established character. Their properties, including unambiguous spin-parity assignments of $1/2^+$, $3/2^+$, $11/2^-$, and $5/2^+$ respectively, were determined from single-proton transfer reactions [13,14,31].

The 2676 keV state is assigned $7/2^-$. It populates both the $11/2^-$ and $1/2^+$ states, fixing the spin-parity to $7/2^-$. The angular correlation of the 993 keV transition with the 1683 keV $E2$ transition [Fig. 3(i)] supports stretched dipole character for the former transition.

The 2709 keV state is assigned $5/2^-$. It populates the $3/2^+$ and $1/2^+$ states only and is populated weakly by higher-lying states, implying low spin. Population by $(9/2^-)$ states from above allows $(5/2, 7/2)^-$. The $\log ft$ result is consistent with unique first-forbidden decay and would be unusually high for first-forbidden decay when compared to the surrounding states. The $5/2^-$ assignment is motivated by the predicted energy of the $\pi s_{1/2}^{-1} \times 3^-$ doublet.

The 2913 keV $(9/2^-)$ state populates the $11/2^-$ state and the $3/2^+$ state. This allows a $7/2^-$ or $9/2^-$ assignment. Due to the strong branching to the $11/2^-$ state and the lack of branching to the $5/2^+$ and $1/2^+$ states, a $9/2^-$ assignment is preferred. The $\log ft$ result is consistent with allowed or first-forbidden decay. Angular correlation of the 2561 keV transition with the 351 keV $M1 + E2$ transition [Fig. 3(ii)] supports the assignment. Angular correlations of the 1564 keV transition with the 423 keV [Fig. 3(iii)] and 446 keV (Ref. [32]) $(M1 + E2)$ transitions feeding from $(9/2^-)$ states are slightly inconsistent with the alternative $7/2^-$ spin-parity assignment.

The 2986 keV $(9/2^-)$ state populates the $11/2^-$ state and the $3/2^+$ state. This allows a $7/2^-$ or $9/2^-$ assignment. Due to the strong branching to the $11/2^-$ state and the lack of branching to the $5/2^+$ and $1/2^+$ states, a $9/2^-$ assignment is preferred. The $\log ft$ result is consistent with allowed or first-forbidden decay. Angular correlation of the 2635 keV $(E3)$ transition with the 351 keV $M1 + E2$ transition [Fig. 3(iv)] is consistent with either assignment.

The 3014 keV $(7/2^-)$ state populates both the $11/2^-$ and $1/2^+$ states. This suggests a $7/2^-$ spin-parity assignment. It also populates the $5/2^+$ state strongly as would be expected for a $J < 9/2$ state. The similarity of these decays to those of the 2676 keV state supports a $7/2^-$ assignment. The angular correlation of the 1331 keV $(E1)$ transition with the 1683 keV $E2$ transition (Ref. [32]) supports stretched dipole character for the former transition.

The 3105 keV $(9/2^-)$ state strongly populates the $11/2^-$ state and the $3/2^+$ state. This allows a $7/2^-$ or $9/2^-$ assignment. Due to the strong branching to the $11/2^-$ state and the lack of branching to the $5/2^+$ and $1/2^+$ states, a $9/2^-$ assignment is preferred. Angular correlations of the 428 keV transition with the 993 keV $(E1)$ transition, and of the 2753 keV transition with the 351 keV $M1 + E2$ transition (Ref. [32]), support a $9/2^-$ assignment.

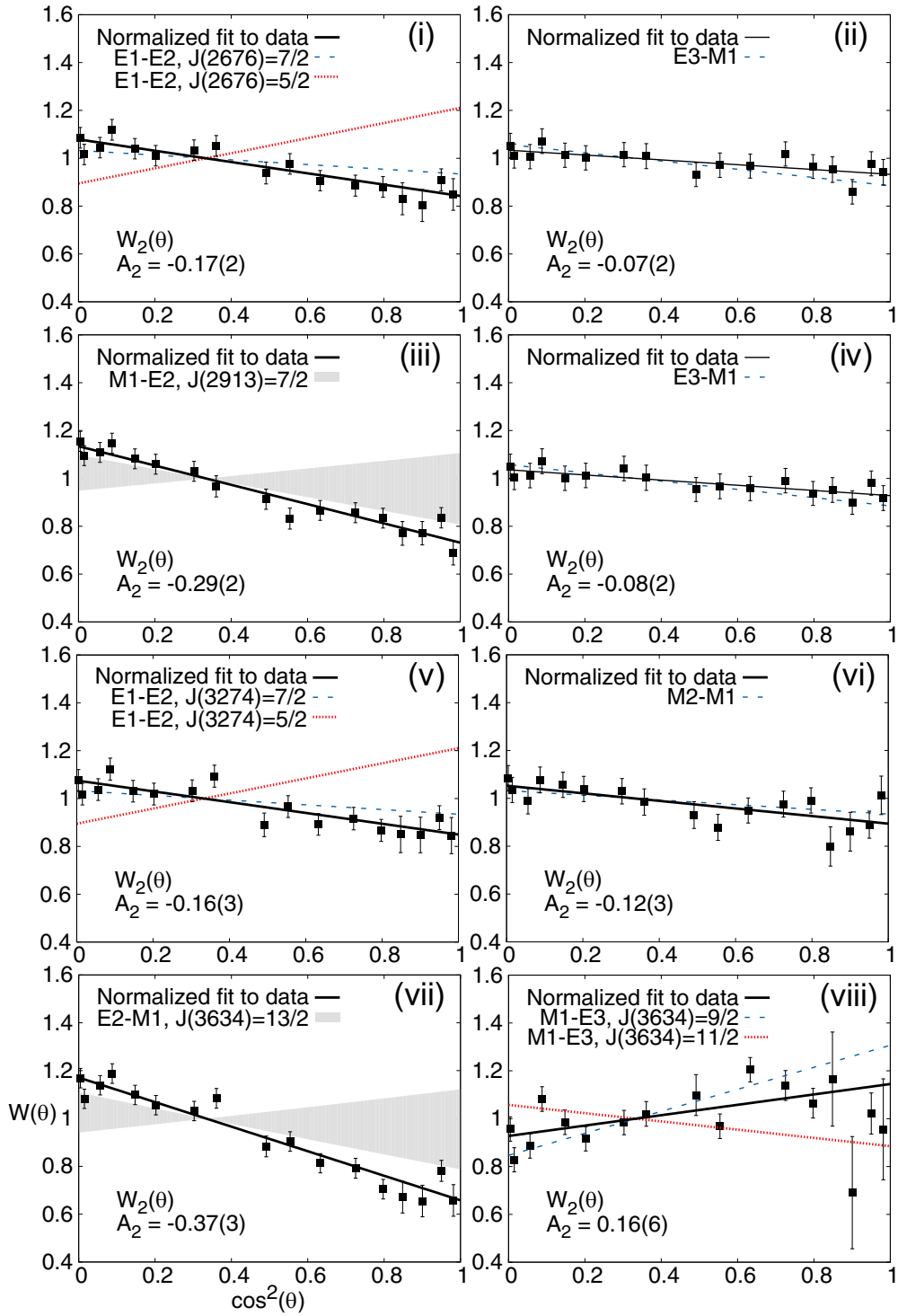

FIG. 3. Examples of angular correlation plots of $W(\theta)$ against $\cos^2(\theta)$ for $\gamma\gamma$ coincidences in ^{207}Tl, discussed in text. Pairs of γ-ray transitions are (i) 993–1683 keV, (ii) 2561–351 keV, (iii) 424–1564 keV, (iv) 2635–351 keV, (v) 1591–1683 keV, (vi) 2922–351 keV, (vii) 648–1638 keV, and (viii) 648–2635 keV. Fit lines are plotted alongside relevant theoretical $W(\theta)$ trends. Shaded regions indicate ranges of possible A_2 values, where mixing ratios of magnetic transitions are unconstrained.

The 3143 keV $(9/2^-)$ state populates the $11/2^-$ state and the $3/2^+$ state. This allows a $7/2^-$ or $9/2^-$ assignment. The branching to the $3/2^+$ state is significantly weaker than for other nearby $(7/2, 9/2)^-$ states, and so a $9/2^-$ assignment is thought to be more likely.

The 3197 keV $(5/2^-)$ state populates the $3/2^+$ state only, suggesting a low spin ($J < 7/2$). It is populated weakly by the $(9/2^-)$ states at 3337 and 3430 keV. This rules against a $J = 3/2$ assignment, leading to $J = (5/2^-)$. The log ft result is also consistent with unique first-forbidden decay.

The 3274 keV $(7/2^-)$ state populates the $11/2^-$ state and the $1/2^+$ state. This allows a $7/2^-$ assignment. The $\log ft$ result is consistent with first-forbidden decay. Angular correlation of the 1591 keV transition with the 1683 keV $E2$ transition [Fig. 3(v)] suggests stretched dipole character for the former, supporting a $7/2^-$ assignment. Angular correlation of the 2922 keV transition with the 351 keV $M1+E2$ transition [Fig. 3(vi)] supports a $7/2^-$ assignment.

The 3296 keV $(9/2^-)$ state populates both the $11/2^-$ and $3/2^+$ states. This allows a $7/2^-$ or $9/2^-$ assignment. A $J=7/2$ assignment is considered unlikely due to the branching ratios of these transitions and the minimal population of low-spin states, leaving $9/2^-$ as the favored assignment.

The 3337 keV $(9/2^-)$ state populates the $11/2^-$ and $3/2^+$ states. This allows a $7/2$ or $9/2^-$ assignment. Angular correlation of the 424 keV transition with the 1564 keV transition [Fig. 3(iii)] is consistent with the assignment.

The 3359 keV $(9/2^-)$ state populates the $11/2^-$ and $3/2^+$ states. This allows a $7/2$ or $9/2^-$ assignment. Angular correlation of the 446 keV transition with the 1564 keV transition (Ref. [32]) is consistent with the assignment.

The 3431 keV $(7/2^-)$ state populates the $11/2^-$ and $3/2^+$ states allowing $J^\pi=(7/2,9/2^-)$. The strength of the transition feeding $11/2^-$ does not support a $7/2^+$ assignment. The relatively large branching ratio of the 1747 keV $(E1)$ transition to the $5/2^+$ state is similar to the $(7/2^-)$ states at 2676 and 3274 keV and so $7/2^-$ is favored for this state.

The 3494 keV $(5/2^-,7/2)$ state populates only the $3/2^+$ state and so $J>7/2$ is ruled out. The $\log ft$ result is too low for second-forbidden decay, restricting the assignment to $J=(5/2^-,7/2)$. The possibility of this state being identical to the 3474(6) keV $7/2^+$ state observed previously [7] has been considered [32] but is thought to be unlikely due to the energy difference.

The 3570 keV $(11/2)$ state is identified only by a transition feeding the $11/2^-$ isomer, thought to indicate $J>9/2$. Its $\log ft$ result is too low for a second-forbidden decay, and is consistent with either an allowed or first-forbidden decay.

The 3581 keV $(9/2^-)$ state populates the $11/2^-$ and $3/2^+$ states allowing $J^\pi=(7/2,9/2^-)$. The lack of branching to $J<7/2$ states favors a $9/2^-$ assignment.

The 3592 keV $(7/2^-)$ state populates the $5/2^+$, $3/2^+$, and $1/2^+$ states along with the 3105 keV $(9/2^-)$ state, allowing $J=(5/2,7/2^-)$. The measured $\log ft$ value is too low for second-forbidden decay. Angular correlation of the 1909 keV transition with the 1683 keV $E2$ transition (Ref. [32]) establishes stretched dipole character for the former, supporting a $7/2^-$ assignment over $5/2^-$.

The 3634 keV $(11/2^-)$ state populates $7/2^-$, $9/2^-$ and $11/2^-$ states. A low $\log ft$ result rules out second-forbidden and unique first-forbidden decay, leaving $J=(7/2,9/2,11/2)$ as possibilities. $J=7/2$ is considered unlikely with no observed branching to $J<7/2$ states. Angular correlations of the 648 keV transition with the 1638 keV $(M1+E2)$ and 2635 keV $(E3)$ transition [Figs. 3(vii), 3(viii)] do not support $13/2^-$ and $11/2^+$ assignments, suggesting $J^\pi=(9/2,11/2^-)$ for this state. Theory predicts multiple $11/2^-$ states to exist in this energy region, so this assignment is preferred.

The 3644 keV $(11/2^-)$ state populates $9/2^-$ and $11/2^-$ states. A low $\log ft$ result rules out second-forbidden and unique first-forbidden decay, leaving $J=(7/2,9/2,11/2)$ as possibilities. $J=7/2$ is considered unlikely with no observed branching to $J<9/2$ states. Theory predicts multiple $11/2^-$ states to exist in this energy region, so this assignment is preferred.

The 3800 keV $(9/2,11/2)$ state populates only $(9/2^-)$ and $11/2^-$ states. The $\log ft$ result rules out second-forbidden and unique first-forbidden decay. The lack of transitions to states of lower spin suggests $J>7/2$, leading to the assignment $J=(9/2,11/2)$. There is a preference for a positive-parity assignment, given that each of the depopulating transitions would be $E1$ in nature. Results from shell model calculations suggest that the $7/2^+, 9/2^+, 11/2^+$ $\pi h_{11/2}^{-1}\times 3^-$ octupole-coupled states lie in this energy region.

The 3850 keV $(7/2,9/2)$ state populates only $(7/2^-)$ and $(9/2^-)$ states and has a $\log ft$ result consistent with allowed or first-forbidden decay, leading to the assignment $J=(7/2,9/2)$.

The 3940 keV $(9/2,11/2)$ state populates a $(9/2^-)$ state and the $11/2^-$ state. The $\log ft$ result rules out second-forbidden and unique first-forbidden decay. The lack of transitions to states of lower spin suggests $J>7/2$, leading to the assignment $J=(9/2,11/2)$.

Our spin-parity assignment is at odds with the most recent Nuclear Data Sheets compilation [7] in some cases. For the 2676 keV state our $7/2^-$ assignment is in agreement with the suggestion of [6]. The $(5/2^+)$ assignment of the compilation is based on the (pol d, ^{3}He) transfer reaction of [13], which reports a small $d_{5/2}$ contribution, however the fit with the experimental data is clearly not good. Similarly, $(9/2)^+$ is suggested by the compilation for the 2986 and 3105 keV states, with the parity assignment based on the $(d,\ ^3\mathrm{He})$ measurement of [12] reporting a $g+10\%d$ component for a group of unresolved states around this energy. In contrast, reference [13] cannot confirm this character. In all three excited states discussed, the misinterpretation was probably due to the (partially) octupole character of these states, with the collective octupole phonon having components from a large number of orbital pairs.

V. SHELL MODEL CALCULATIONS

The experimental findings are compared to shell model calculations using the KHM3Y interaction. The latter has previously been successful in describing the octupole phonon (and double octupole excitation) in ^{208}Pb [5] and in describing nuclei consisting of the ^{208}Pb core plus several particles and/or holes [33]. The calculation has previously been applied to ^{207}Tl and compared to the findings of an experiment studying high-energy yrast states [4].

A large model space is used around the ^{208}Pb shell gaps, covering the ranges $Z=50$–126, $N=82$–184. The proton model space includes the orbitals $1g_{7/2}$, $2d_{5/2}$, $1h_{11/2}$, $2d_{3/2}$, and $3s_{1/2}$ below $Z=82$ and $1h_{9/2}$, $2f_{7/2}$, $1i_{13/2}$, $2f_{5/2}$, $3p_{3/2}$, and $3p_{1/2}$ above. The neutron model space includes the orbitals $2f_{7/2}$, $1h_{9/2}$, $3p_{1/2}$, $2f_{5/2}$, $3p_{3/2}$, and $1i_{13/2}$ below $N=126$ and $2g_{9/2}$, $1i_{11/2}$, $1j_{15/2}$, $3d_{5/2}$, $4s_{1/2}$, $2g_{7/2}$, and

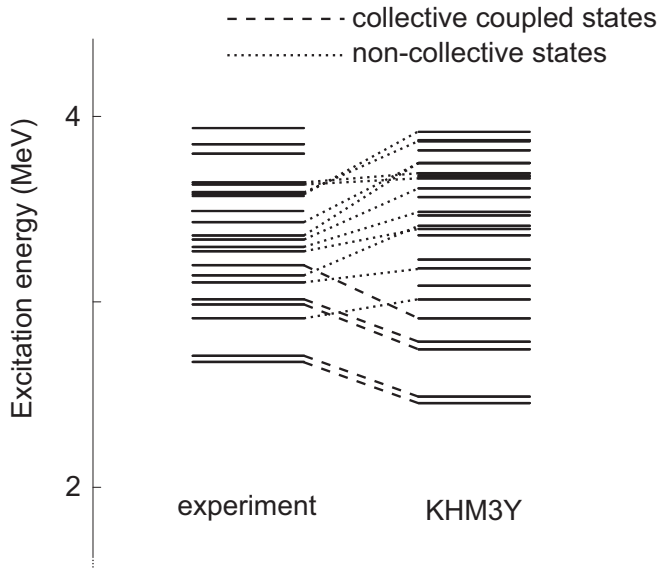

FIG. 4. Comparison of experimentally observed level energies in ^{207}Tl with those predicted by calculations using the KHM3Y interaction, described in the text. Single-particle states are not shown as these were fixed in calculations. Character assignments for collective octupole and noncollective states are shown.

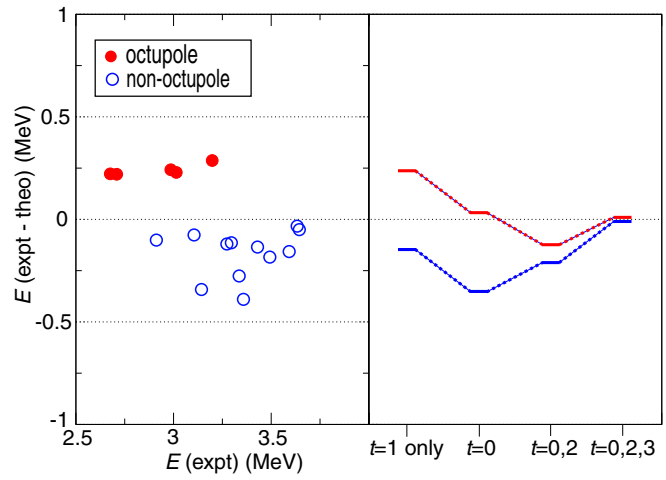

FIG. 5. Left: difference between experimental and calculated state energies (character assignments discussed in text). Right: estimated effect (not to scale) on average energy differences when including mixing with different numbers of core excitations, t, in the calculation. The first point corresponds to the $t = 1$ truncation used in the analysis.

$3d_{3/2}$ above. Cross-shell two-body matrix elements (TBMEs) are based on the M3Y interaction [34], and neutron-proton particle-particle and hole-hole TBMEs use the Kuo-Herling interaction [35] as modified in Ref. [33].

Relative to a closed-shell configuration for ^{208}Pb, the configurations were truncated to have one-hole (1h) π^{-1} ($t = 0$), or one-particle two-hole (1p-2h) $\pi^{1}\pi^{-2}$ and $\nu^{1}\pi^{-1}\nu^{-1}$ ($t = 1$). Mixing between $t = 0$ and $t = 1$ was not taken into account. With this truncation the single-particle and single-hole energies are given by experimental separation energies for $A = 207$ and $A = 209$ relative to ^{208}Pb as shown in Fig. 1 of [33].

VI. DISCUSSION

The relation of the experimental level scheme to calculated levels is shown in Fig. 4. The differences between experimental and theoretical state energies are plotted in Fig. 5. We discuss octupole state assignments here.

The pair of states at 2676 and 2709 keV has previously been assumed [6,9] to correspond to the doublet of $\pi s_{1/2}^{-1} \times 3^-$ octupole-coupled states owing to their energies and tentative spin-parities. This analysis supports the tentative assignments and asserts the octupole character. As further evidence supporting the respective $7/2^-$ and $5/2^-$ spin-parity assignments, the relative strengths of the $E1$ and $E3$ transitions depopulating these states agree with those calculated by Hamamoto [36]. Experimentally and theoretically the states are separated in energy from the states lying above by around 200 keV. These states are predicted by the KHM3Y calculation to lie at 2453 and 2489 keV respectively. This gives respective observed energy shifts $\Delta E_{\mathrm{M3Y}} = E_{\mathrm{exp.}} - E_{\mathrm{KHM3Y}} = +0.223$ and $+0.256$ MeV.

Placing the $\pi d_{3/2}^{-1} \times 3^-$ octupole-coupled states is less clear and so remains tentative. These have spin-parities $3/2^-$, $5/2^-$, $7/2^-$, and $9/2^-$, and would be expected to lie close to 3 MeV in energy if coupling is weak as for the $\pi s_{1/2} \times 3^-$ states. The strength of the transition directly deexciting the coupled phonon state (populating the $3/2^+$ state at 351 keV) is expected to be stronger than the corresponding transition for a noncollective state. KHM3Y shell model calculations predict state energies, transition strengths and wave functions. The wave functions clearly differentiate between calculated octupole and non-octupole states, with octupole state wave functions dominated by contributions from $\Delta l = \Delta j = 3$ excitations across the shell gaps.

The search for the $3/2^-$ and $5/2^-$ $d_{3/2}$ octupole-coupled states is hindered by a lack of statistics due to both lower spin and greater β-decay forbiddenness. Apart from the $5/2^-$ state at 2709 keV, these two are the only $J < 7/2$ states expected to exist between 2.5 and 3.5 MeV in energy. A single candidate state is observed: the 3197 keV state is assigned $(5/2^-)$ here. It is thought that the $3/2^-$ state remains unobserved, populated negligibly in β decay and with very little internal population from higher-spin states lying above. The $5/2^-$ state is predicted by the KHM3Y calculation to lie at an energy of 2911 keV, giving an observed energy shift $\Delta E_{\mathrm{M3Y}} = +0.286$ MeV.

Four $(7/2^-)$ states are observed above the $7/2_1^-$ state, lying at 3014, 3274, 3431, and 3592 keV. The $7/2_2^-$ state is predicted by the KHM3Y calculations to have octupole character and to lie at an energy of 2784 keV. Experimentally this would correspond to the 3014 keV state, but the 3274 keV state is also considered based on its energy. Each of the $(7/2^-)$ states populates the $5/2^+$ state at 1683 keV with an $(E1)$ transition and the $\pi d_{3/2}^{-1}$ state at 351 keV with an $(M2 + E3)$ transition. The latter would be expected to

be enhanced for the octupole state. The relative transition strength of the $(M2 + E3)$ transition from the 3014 keV state, when using the $(E1)$ transition as a benchmark, is around 60% greater than that of the corresponding transition from the 3274 keV state. This supports tentative assignment of collective octupole character to the 3014 keV state, and given the relative energies of the states, this appears likely. However, it is also possible that the octupole strength might instead be split, most likely between the 3014 and 3274 keV states, rather than concentrated in one state as predicted by the KHM3Y calculation. This could be attributed to the underestimation of the octupole energy by several hundred keV: the energy difference $E(7/2_3^-) - E(7/2_2^-)$ is calculated to be 0.61 MeV whereas it is observed to be 0.26 MeV. As the octupole states are higher in energy than predicted by the calculations, they are closer to the multitude of states with equal J^π, increasing the degree of mixing.

The density of observed $9/2^-$ states (eight placed in the energy range 2.9–3.5 MeV) makes exact assignment difficult, with increased uncertainty over predicted configuration mixing. The KHM3Y calculations predict the $9/2_1^-$ state to have octupole character, which here would correspond to the 2913 keV state. The 2986 and 3105 keV states are considered to be the next most likely candidates owing to energy ordering and strong octupole-de-exciting transitions. Each of these three states populates both the $11/2^-$ isomer with an $M1 + E2$ transition and the $3/2^+$ $\pi d_{3/2}^{-1}$ state with an $E3$ transition. Calculation of octupole relative transition strengths, using the isomer-populating $M1 + E2$ transition as a benchmark, suggests that the 2635 keV transition (depopulating the 2986 keV state) is the strongest. This supports tentative assignment of $d_{3/2}$-coupled octupole character to the 2986 keV state. However, as for the $7/2^-$ states, this is not robust evidence. The phonon strength could also be split between the three states at 2913, 2986, and 3105 keV. $E(9/2_2^-) - E(9/2_1^-)$ is calculated to be 0.27 MeV whereas it is observed to be 0.07 MeV.

The final octupole-coupled states considered are the $\pi h_{11/2}^{-1} \times 3^-$ states. Of those expected to be populated, the $7/2^+$ state is calculated to lie the lowest in energy, at 3679 keV, with the $9/2^+$ and $11/2^+$ states lying around 100–200 keV higher. The $17/2^+$ state has been observed at 3813 keV [4], giving $\Delta E_{\mathrm{M3Y}} = +0.132$ MeV. This is in line with results for $\pi s_{1/2}^{-1}$, $\pi d_{3/2}^{-1}$ coupled states in this analysis. The observed 3800, 3850, and 3940 keV states are not assigned parity and lie in this energy region, and so are candidates for octupole character. Previously a state at 3987 keV, not observed in this work, was assigned $L = 4$ and some $\pi g_{7/2}^{-1}$ strength [13], making this more likely to correspond to the $7/2^+$ octupole-coupled state.

Characterization of states not resulting from octupole coupling here is difficult as they are less easy to identify through any particular multipole enhancement. The experimentally observed states with tentative spin-parities not assigned octupole character are assigned to calculated states in order of energy. The 3634 and 3644 keV $(11/2^-)$ states are assigned to the calculated $11/2_4^-$ and $11/2_5^-$ states due to the similarities in energy separation. The states at 3494, 3570, 3800, 3850, and 3940 keV are not assigned exact spin-parities.

Figure 5 shows that the KHM3Y calculations consistently underestimate the energy of the octupole phonon states by around 0.25 MeV and overestimate the energy of other coupled states by around 0.2 MeV. The energy of the 3813 keV $17/2^+$ state in ^{207}Tl observed in a previous experiment [4] was also underestimated by 0.13 MeV. When the results of the calculation are compared with known single-octupole-coupled states in nuclei adjacent to ^{208}Pb [1,7,29], all energies are underestimated by between 0.0 and 0.3 MeV.

The differences between theory and experiment are probably related to the truncation made in the calculations. As a start, mixing between $t = 0$ and $t = 1$ should be taken into account. This was not done since it requires the determination of a new Hamiltonian in which all of the single-particle energies are readjusted to reproduce the experimental separation energies for $A = 207$ and $A = 209$ relative to ^{208}Pb. This, of course, requires calculations for all of these nuclei. Mixing between $t = 0$ and $t = 1$ lowers the energies of the states dominated by $t = 0$, i.e., they get pushed down due to mixing with the higher energy 1p-2h states. This will increase the relative energies of the $t = 1$ states. Mixing with $t = 2$ states is expected to reduce the energies of the $t = 1$ states, but would also reduce the energy of the ground state as 0^+ nucleon pairs are easier to excite across the shell gap. Finally, mixing with $t = 3$ states would be expected to reduce the energies of $t = 1$ states. It is likely that $t = 2$ (2p-3h) and $t = 3$ (3p-4h) would be needed to achieve energy convergence at the level of about 100 keV. A previous investigation in the smaller model space around ^{98}Cd [37] found that the inclusion of mixing up to $t = 3$ is necessary to ameliorate the difference between measurement and theory. Including this amount of configuration mixing for the region around ^{208}Pb is not computationally feasible at this time.

To address the discrepancy between octupole and non-octupole predictions in this analysis, the $t = 2$ mixing would need to have a relatively smaller effect on the collective octupole-coupled states. The mechanism for this difference is not clear, although it could relate to weak coupling of the collective phonon with $t = 0$ states. Spin is not thought to have a significant effect, since these states are all of similar, relatively low spin. Wilson *et al.* discussed the rectifying effect of $t = 2$ mixing on high-spin states [4].

VII. CONCLUSIONS

The γ-decay scheme of ^{207}Tl has been investigated following population through β decay from the $J^\pi = (9/2^+)$ ground state in ^{207}Hg. An extended level scheme has been established containing several newly observed states and transitions and through a combination of approaches, including angular-correlation measurements, spin-parities have been suggested for most states. States resulting from coupling between $t = 0$ single-proton-hole states and the collective octupole phonon have been identified where possible. Comparison with the results of state-of-the-art shell model calculations, using an extensive model space, indicate a discrepancy between the energy predictions of octupole-coupled states and other non-collective coupled states. This is also the case for collective

states observed in other nuclei neighboring ^{208}Pb [1,7,29]. We speculate that a reduction in the degree to which the collective states couple to $t = 2$ excitations could resolve this difference.

ACKNOWLEDGMENTS

The research leading to these results has received funding from the European Union's Horizon 2020 Research and Innovation Programme under Grant Agreement No. 654002. Support from the European Union Seventh Framework through ENSAR Contract No. 262010, the Science and Technology Facilities Council (UK), the MINECO Projects No. FPA2015-64969-P and No. FPA2017-87568-P (Spain), FWO-Vlaanderen (Belgium), GOA/2015/010 (BOF KU Leuven), the Excellence of Science Programme (EOS-FWO), the Interuniversity Attraction Poles Programme initiated by the Belgian Science Policy Office (BriX network P7/12), the German BMBF under Contract No. 05P18PKCIA + "Verbundprojekt 05P2018," the Polish National Science Centre under Contracts No. UMO-2015/18/M/ST2/00523 and No. UMO-2019/33/N/ST2/03023, the National Science Foundation (US) Grant No. PHY-1811855 and the Romanian IFA project CERN-RO/ISOLDE is acknowledged. P.H.R. and S.M.J. acknowledge support from the UK Department for Business, Energy and Industrial Strategy via the National Measurement Office.

[1] M. J. Martin, Nucl. Data Sheets **108**, 1583 (2007).
[2] M. Rejmund *et al.*, Eur. Phys. J. A **8**, 161 (2000).
[3] Zs. Podolyák *et al.*, J. Phys.: Conf. Ser. **580**, 012010 (2015).
[4] E. Wilson *et al.*, Phys. Lett. B **747**, 88 (2015).
[5] B. A. Brown, Phys. Rev. Lett. **85**, 5300 (2000).
[6] B. Jonson *et al.*, CERN Report No. 81-09, 1981 (unpublised), p. 640.
[7] F. G. Kondev and S. Lalkovski, Nucl. Data Sheets **112**, 707 (2011).
[8] G. Wang *et al.*, Chin. Phys. C **41**, 030003 (2017).
[9] O. Hansen *et al.*, Nucl. Phys. A **127**, 71 (1969).
[10] P. Barnes *et al.*, Phys. Rev. C **1**, 228 (1970).
[11] E. R. Flynn *et al.*, Nucl. Phys. A **279**, 394 (1977).
[12] H. Langevin-Joliot *et al.*, J. Phys. G: Nucl. Phys. **10**, 1435 (1984).
[13] P. Grabmayr *et al.*, J. Phys. G **18**, 1753 (1992).
[14] I. Bobeldijk *et al.*, Phys. Lett. B **356**, 13 (1995).
[15] M. Hunyadi *et al.*, Nucl. Phys. A **731**, 49 (2004).
[16] R. Bailey, CERN Report No. 2013-007, 2013 (unpublished), p. 331.
[17] A. I. Morales *et al.*, Phys. Rev. C **84**, 011601(R) (2011).
[18] Zs. Podolyák *et al.*, Phys. Rev. Lett. **117**, 222302(R) (2016).
[19] N. Warr *et al.*, Eur. Phys. J. A **49**, 40 (2013).
[20] H. Scraggs *et al.*, Nucl. Instrum. Methods Phys. Res., Sect. A **543**, 431 (2005).
[21] I. Lazarus *et al.*, IEEE Trans. Nucl. Sci. **48**, 567 (2001).
[22] H. W. Taylor *et al.*, Nucl. Data Tables **A9**, 1 (1971).
[23] M. E. Rose, Phys. Rev. **91**, 610 (1953).
[24] T. A. Berry, Ph.D. thesis, University of Surrey, 2019 (unpublished).
[25] S. Gorodetzky, F. Beck, and A. Knipper, Nucl. Phys. **82**, 275 (1966).
[26] T. Kibédi *et al.*, Nucl. Instrum. Methods Phys. Res., Sect. A **589**, 202 (2008).
[27] B. Singh *et al.*, Nucl. Data Sheets **84**, 487 (1998).
[28] M. Kadi, P. E. Garrett, M. Yeh, S. W. Yates, T. Belgya, A. M. Oros-Peusquens, and K. Heyde, Phys. Rev. C **61**, 034307 (2000).
[29] J. Chen and F. Kondev, Nucl. Data Sheets **126**, 373 (2015).
[30] F. G. Kondev, Nucl. Data Sheets **109**, 1527 (2008).
[31] R. Neveling, A. A. Cowley, G. F. Steyn, S. V. Frtsch, G. C. Hillhouse, J. Mano, and S. M. Wyngaardt, Phys. Rev. C **66**, 034602 (2002).
[32] T. A. Berry *et al.*, Phys. Lett. B **793**, 271 (2019).
[33] E. K. Warburton and B. A. Brown, Phys. Rev. C **43**, 602 (1991).
[34] G. Bertsch *et al.*, Nucl. Phys. A **284**, 399 (1977).
[35] G. H. Herling and T. T. S. Kuo, Nucl. Phys. A **181**, 113 (1972).
[36] I. Hamamoto, Nucl. Phys. A **205**, 225 (1973).
[37] A. Blazhev *et al.*, Phys. Rev. C **69**, 064304 (2004).